

## Research Article

**Deformation Characteristics of Basalt Fiber Reinforced Recycled Aggregate Concrete after High Temperature****Xianggang Zhang<sup>1,2,3</sup>, Xuyan Liu<sup>2</sup>, Youchuan Shen<sup>2</sup>, Shuren Wang<sup>2,\*</sup> and Qianqian Liu<sup>2</sup>**<sup>1</sup>State Key Laboratory of Building Safety and Built Environment, Beijing 100013, China<sup>2</sup>International Joint Research Laboratory of Henan Province for Underground Space Development and Disaster Prevention, Henan Polytechnic University, Jiaozuo 454003, China<sup>3</sup>National Engineering Research Center of Building Technology, Beijing 100013, China

Received 3 January 2022; Accepted 19 May 2022

**Abstract**

To examine how basalt fiber reinforced recycled aggregate concrete (BFRRC) deforms after being exposed to high temperatures, the deformation characteristics tests were conducted on 81 standard prismatic specimens with replacement ratios of recycled coarse aggregate (RCA) (0%, 50%, and 100%), basalt fiber (BF) dosage (0 kg/m<sup>3</sup>, 2 kg/m<sup>3</sup>, and 4 kg/m<sup>3</sup>), and temperature (25 °C, 300 °C, and 600 °C) as the variation parameters. The variation factors on deformation characteristics such as elastic modulus and Poisson's ratio of BFRRC were discussed. The analytical expressions of the elastic modulus of BFRRC with different variation parameters after high-temperature treatment were proposed. Results show that the elastic modulus gradually decreases with the increasing of replacement ratio and temperature, and gradually increases with the increasing of BF dosage. The increase of Poisson's ratio is primarily concentrated between 300 °C and 600 °C, and the 100% replacement ratio of recycled aggregate has the greatest influence on the Poisson's ratio. The variation parameters on Poisson's ratio are opposite to that of the elastic modulus. The conclusions obtained in this study provide a significant reference for design and application of BFRRC after high temperature.

**Keywords:** Recycled coarse aggregate, Basalt fiber, High temperature, Elastic modulus, Poisson's ratio

**1. Introduction**

The rapid growth of the global construction sector not only consumes a vast amount of natural resources, but also pollutes the environment and produces the greenhouse effect and ozone layer depletion [1, 2]. According to statistics, the annual output of construction waste in China has reached 1.8 billion tons and is increasing every year [3]. Only 5% of construction waste is recycled, and the rest is buried in the ground, even though China will consume a considerable amount of sand, stone, and other aggregates in future buildings, causing pollution and depletion of restricted natural resources through mining alone [4, 5]. The recycling and utilization of waste concrete is a major problem faced by scientific researchers and engineers due to the rapid increase in the amount of waste concrete and the limited supply of natural aggregates [6, 7]. Recycled Aggregate Concrete (RAC) technology can effectively maximize the utilization of construction waste, meet the huge demand for sand and stone aggregates in infrastructure construction, promote construction industry's transformation to a circular economy model, and fundamentally eliminate rapid development at the expense of the environment [8, 9].

Natural aggregates are partially replaced with recycled aggregates in concrete mixtures to make recycled aggregate concrete, which has major environmental and economic benefits [10]. However, the use of recycled aggregates in concrete constructions is still in its early stages, necessitating specialized treatment methods to improve the material's poor

mechanical qualities, resulting in high production costs. As a result, selecting an effective approach to improve the mechanical properties of RAC is critical. By incorporating a particular quantity of BF into RAC, the brittleness of the cement matrix can be improved, allowing for modification and the formation of BFRRC. The BF in BFRRC has a toughening and crack resistance effect, limiting the formation and expansion of internal micro-cracks under stress, providing it superior compression, crack resistance, ductility, and energy dissipation qualities over RAC [11-14].

Improving the mechanical properties of RAC with BF modification has now become a feasible and useful research approach, and BFRRC research by domestic and international researchers is growing every year [15]. However, the majority of the study is focused on normal temperature qualities, with only a few studies focusing on high temperature properties. The high temperature test of BFRRC and the experimental investigation of BFRRC deformation performance after high temperature treatment are carried out in this paper, which is important for BFRRC use in engineering construction.

**2. State of the Art**

Many studies have shown that fiber can increase the strength of concrete because of the bridging effect on the creation and expansion of cracks, and improve the ductility of concrete. Several types of fiber can add to concrete, including steel fiber, glass fiber, carbon fiber, and organic fiber. For examples, Gao et al. [16] investigated the shear performance of steel fiber concrete beams and the results showed the shear load capacity of the beams gradually increased with the increasing of the

\*E-mail address: w\_sr88@163.com

ISSN: 1791-2377 © 2022 School of Science, IHU. All rights reserved.

doi:10.25103/jestr.152.11

volume fraction of steel fiber. Liu et al. [17] studied the flexural performance of steel fiber reinforced recycled aggregate concrete-filled tube columns, and the results revealed the steel fiber improved the flexural capacity, while an optimum steel fiber volume fraction of 1.2% was recommended. Meesala [18] studied the effect of different fiber types on the mechanical properties of RAC and ordinary concrete. The results proved that fiber significantly improved the mechanical properties of ordinary concrete and RAC, with the greatest effect on steel fiber. Ali et al. [19] proposed a new method of adding glass fiber and fly ash to improve the mechanical properties and durability of RAC. They found that the use of glass fiber improved the mechanical properties of RAC, but also increased the water absorption and chloride permeability. Xiong et al. [20] examined the effect of glass fiber on the compressive strength of concrete and they found that adding glass fiber significantly could improve the compressive strength of concrete. Samani and Lak [21] explored the mechanical properties of waste carbon fiber reinforced recycled aggregate concrete. They found that adding carbon fiber to concrete could improve the mechanical properties of concrete and prevent the expansion of initial cracks, increase the ductility and energy dissipation capacity of concrete.

Some scholars, such as Ding et al. [22] studied the flexural performance of concrete with the addition of carbon fiber and revealed that carbon fiber could improve the flexural strength of concrete. Lee [23] researched the effect of nylon fiber on the permeability and mechanical properties of concrete. The results showed that adding nylon fiber in RAC could improve the performance of concrete, and the higher the nylon fiber content, the stronger the mechanical properties and permeability of concrete. Sainz-Aja et al. [24] searched the effect of polyethylene fiber on concrete properties. It was found that the mechanical properties of concrete improved with the addition of fiber, especially the tensile strength, as well as excellent performance in controlling concrete cracking. Kim et al. [25] studied the strength and ductility of polyethylene fiber reinforced concrete components and showed that the compressive strength and elastic modulus decreased with increasing fiber volume fraction and the ductility increased significantly. However, these fibers have several disadvantages such as high-density, high cost, and low chemical resistance, which reduce the workability of concrete [26]. BF, a synthetic fiber with excellent properties, has a production similar to that of alkali-free glass fiber, but with lower production costs and without chemical additives [27]. At the same time, BF also has excellent properties such as lightweight, high temperature resistance, good chemical stability, nontoxicity and environmental protection, and good compatibility with RAC [28]. Therefore, it is important to study incorporating BF into RAC to form BFRRc.

The other scholars are concentrating their efforts on the basic mechanical properties of BFRRc at room temperature. Alnahhal and Aljidda [29] investigated the influence of the BF volume fraction and the RCA replacement ratio on the flexural strength of BFRRc in an experimental investigation. The effect of the RCA replacement ratio on the flexural strength of BFRRc was not significant, and the flexural strength improved as the BF dosage increased. Dong et al. [30] tested BFRRc's mechanical qualities, examined all elements of its mechanical properties, and came to the conclusion that BF can improve RAC's mechanical properties. Zhang et al. [31] investigated the impact of RCA replacement ratio and BF dosage on the mechanical properties of RAC, finding that when the replacement ratio was 50%, the basic mechanical

qualities of RAC with various BF dosages were superior to conventional concrete. Huang et al. [32] investigated the influence of BF dosage and RCA replacement ratio on the mechanical characteristics of concrete. They found that when the RCA replacement ratio was increased, the compressive and flexural strengths of RAC reduced at first, then slightly increased, but the splitting tensile strength remained constant. The flexural and splitting tensile strengths of RAC grew dramatically as the fiber dosage increased, but the compressive strength first increased and subsequently declined.

The past studies have mainly focused on qualities at room temperature, with only a few studies focusing on properties at high temperatures. Experimental studies on BFRRc specimens after the high temperature is conducted in this paper to investigate the effect of temperature, fiber dosage, and replacement ratio on their elastic modulus and Poisson's ratio, as well as to establish relevant expression to serve as a reference for future BFRRc research and application.

The rest of this study is organized as follows. Section 3 describes the experimental design. Section 4 quantitatively analyzes the elastic modulus and Poisson's ratio, and finally, the conclusions are summarized in Section 5.

### 3. Methodology

#### 3.1 Test material

In the tests, P-O 42.5R grade cement with fineness, loss of ignition, compressive strength, flexural strength, and initial/final setting time of 1.3%, 2.4%, 50 MPa, 8 MPa, and 185/270 min was used, respectively. Fly ash with a grade, fineness, density, water content, and loss of ignition of grade II, 45  $\mu\text{m}$ , 2.4  $\text{g}/\text{cm}^3$ , 0.25%, and 2.4%, was used respectively, and its dosage was 20% of the cement dosage. Brown-yellow solid water reducing agent with a water reduction of 15% - 25% was used, and its dosage was 0.5% of the cementitious materials (cement and fly ash). Short-cut basalt fibers with an outer diameter of 15  $\mu\text{m}$ , a length of 18 mm, and a density of 2650  $\text{kg}/\text{m}^3$  were utilized, with tensile strength, elastic modulus, and elongation at break of 4500 MPa, 104 GPa, and 3.1%, respectively. The natural coarse aggregate was made of well-graded natural gravel; the recycled coarse aggregate was obtained by mechanical crushing from a waste concrete pavement, and after washing and drying for 72 h, the recycled coarse aggregate with particle sizes of 5-20 mm and 10-30 mm was mixed in a mass 3:2 ratio to ensure continuous gradation. According to the Pebble and Crushed Stone for Construction (China GB/T 14685-2011), the measured basic physical properties of coarse aggregate are listed in Table 1. Sun-dried natural yellow sand with apparent density, bulk density, porosity, and fineness modulus of 2600  $\text{kg}/\text{m}^3$ , 1300  $\text{kg}/\text{m}^3$ , 50.29%, and 2.16, was used as the fine aggregate, respectively.

#### 3.2 Mix proportions of RAC

According to the Specification for mix proportion design of ordinary concrete (China JGJ 55-2011), BFRRc's test mix strength was C40. To begin, the appropriate water-binder ratio and the amount of each material were determined. Next, the mix proportions were designed under the three working conditions of 0%, 50%, and 100%, respectively, based on the percentage of recycled coarse aggregate to the mass of all coarse aggregate, and the amount of additional water was considered based on the amount of recycled coarse aggregate,

water content, and water absorption. The test design RAC mix proportions are listed in Table 2.

**Table 1.** Basic physical properties of coarse aggregate.

Name	Particle size (mm)	Bulk density (kg/m <sup>3</sup> )	Apparent density (kg/m <sup>3</sup> )	Water content (%)	Water absorption (%)	Crushing index
Natural aggregate	5-30	1681	2798	0.7	0.1	10.4
Recycled aggregate	5-30	1274	2433	1.8	3.5	12.7

### 3.3 Parameter design and specimen preparation

A total of 27 sets of specimens were designed to study the effects of variation parameters such as recycled coarse aggregate replacement ratio ( $\delta$ ), basalt fiber dosage ( $\lambda$ ), and temperature ( $T$ ) on the deformation properties of BFRRC. The replacement ratio of recycled coarse aggregate was tested under three conditions: 0%, 50%, and 100%, and the basalt fiber dosage was tested under three conditions: 0 kg/m<sup>3</sup>, 2

kg/m<sup>3</sup>, and 4 kg/m<sup>3</sup>, and the temperature was tested under three conditions: 25 °C, 300 °C, and 600 °C. The specimens were created in a group of three to minimize test error, and a total of 81 standard prismatic specimens measuring 150 mm × 150 mm × 300 mm were made for the elastic modulus and Poisson's ratio tests.

**Table 2.** Mix proportions of recycled aggregate concrete.

$\delta$ (%)	W/B	$S_s$ (%)	$m_w$		$m_B$		$m_A$		$m_s$	$m_{wra}$
			$m_{nw}$	$m_{aw}$	$m_c$	$m_{FA}$	$m_r$	$m_n$		
0	0.47	32	191	0.0	346	60.9	0.0	1224.9	577	2.04
50	0.47	32	191	10.0	346	60.9	612.4	612.4	577	2.04
100	0.47	32	191	20.0	346	60.9	1224.9	0.0	577	2.04

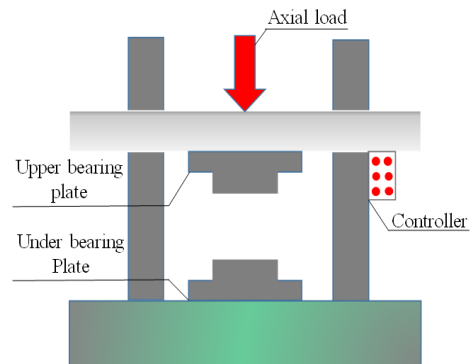
Note W/B is the water-binder ratio;  $\delta$  is the replacement ratio of recycled coarse aggregate;  $S_s$  is the sand ratio;  $m_{nw}$ ,  $m_{aw}$  are the amount

According to the Standard for test methods of concrete physical and mechanical properties (China GB/T50081-2019), the samples were molded in standard molds and left to stand for 24 h after pouring, vibrating, compacting, and smoothing, following which they were uniformly placed in a standard curing environment (20 ± 2 °C, relative humidity > 95%) to match the specimens' molding quality. The above tests were done within the standard age after 28 d of specimen upkeep to assure the data's accuracy.

### 3.4 Test method

The standard specimens after different high temperatures treatment were subjected to BFRRC deformation performance tests. Strain gauges were to be attached at the vertical midline of the three sides of the standard prismatic specimen for the elastic modulus and Poisson's ratio tests, and the strain gauges had to be centered with each other. The loading device adopted a WAW-2000 microcomputer-controlled electro-hydraulic servo universal test machine with a measuring range of 2000 kN, which made the failure load value of the BFRRC specimen located within 20% -80% of the total measuring range of the press to ensure the accuracy of the test results. The schematic diagram of the loading device is shown in Fig. 1.

The specimen needs to be preloaded before loading to assure the accuracy of the test, reduce the uneven surface of the specimen, the gap between the loading surface, and the lack of stiffness of the compression testing machine at the start of loading. According to the Standards for test methods of concrete physical and mechanical properties (China GB50081-2019), the loading rate of the elastic modulus and Poisson's ratio test was set at 0.5 MPa/s, the benchmark load value  $F_0$  was 0.5 MPa, the maximum preload value  $F_a$  was 1/3 of the axial compressive strength of the specimen, and after the preload centering, three repeated preloads were carried out between the two values of  $F_0$  and  $F_a$ , loaded to  $F_0$  and  $F_a$  for the 60 s with a constant load, and recorded the deformation value of each measurement point, and then calculated the elastic modulus and Poisson's ratio. The loading method for the elastic modulus and Poisson's ratio tests is shown in Fig. 2.



(a) Compression testing machine



(b) Monitoring points

**Fig. 1.** The schematic diagram of the loading device

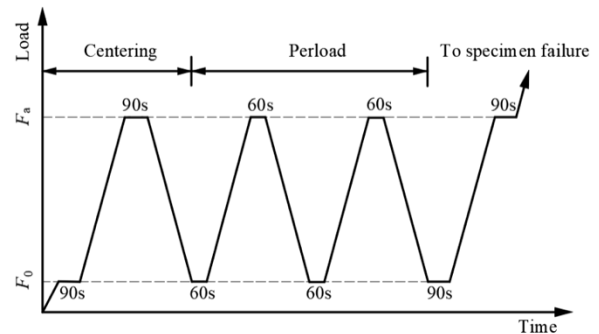


**Fig. 2.** Schematic diagram of loading method.

#### 4. Results analysis and discussion

##### 4.1 Elastic modulus

##### 4.1.1 Analysis of influencing factors of elastic modulus

A histogram of the measured values of the elastic modulus of the specimens is presented in Fig. 3. The elastic modulus of the specimens with single parameter temperature fluctuation reduced dramatically after experiencing high temperature influence, as shown in Fig. 3. With the same fiber dosage and replacement ratio, the decreased range of elastic modulus was between 37.8% and 52.9% when the temperature was raised from 25 °C to 300 °C; when the temperature was raised from 300 °C to 600 °C, the decreased range of elastic modulus was between 62.7% and 66.1% when the temperature was raised from 300 °C to 600 °C. This is because the specimen becomes loose and multi-holed within after the high temperature effect, and there are a great number of microcracks, which are generated by excessive deformation of the specimen during the loading process.

The elastic modulus of the specimens with single parameter change of replacement ratio exhibited a declining trend as the replacement ratio increased. At the same temperature and fiber dosage, the decreased range of elastic modulus was between 13.3% and 29% when the replacement ratio was increased from 0% to 50%; when the replacement ratio was increased from 50% to 100%, the decreased range of elastic modulus was between 15% and 28.7%. This is due to the low stiffness of recycled aggregates with high porosity, as well as the fact that the old mortar adhered to its surface reduces the density of the specimen, causing the elastic modulus to fall as the replacement ratio increases.

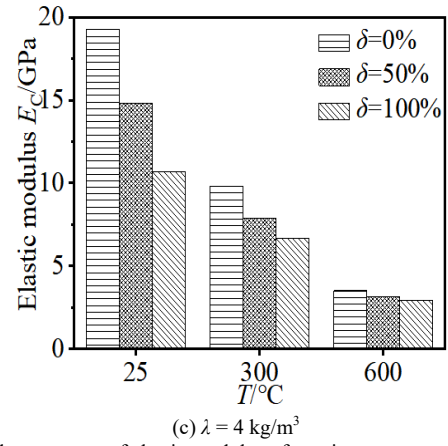
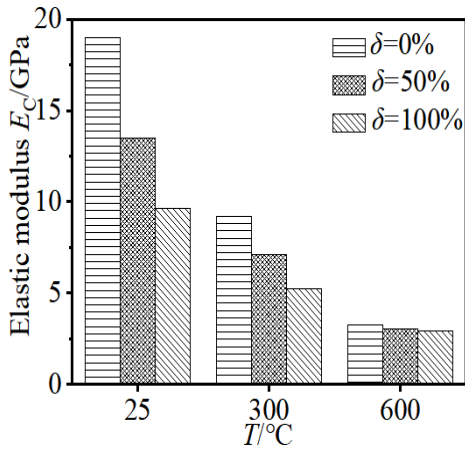


Fig. 3. Change range of elastic modulus of specimens.

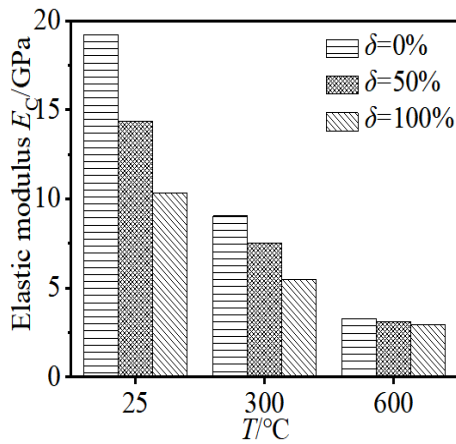
The elastic modulus of the specimens with a single parameter modification of fiber dosage gradually increased as the BF concentration increased. When the BF dosage was increased from 0 to 2 kg/m<sup>3</sup>, the elastic modulus of the specimens increased between 2% and 8% at the same temperature and replacement ratio; when the BF dosage was increased from 2 to 4 kg/m<sup>3</sup>, the elastic modulus of the specimens increased between 1.1% and 7.4% at the same temperature and replacement ratio. This is because BF is more compatible with RAC, and introducing a small quantity of BF into the specimen can increase its density, enhancing its elastic modulus. Because the deformation of the specimen is minor in the elastic stage, and the bridging action of BF in the RAC plays little part in this process, the improvement is not significant.

##### 4.1.2 Functional relationship among elastic modulus and different parameters

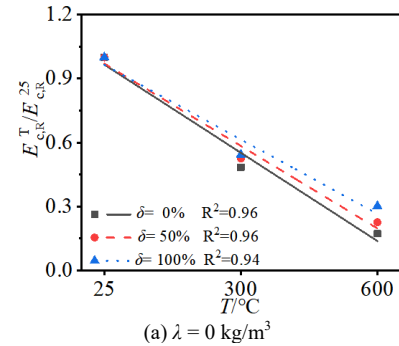
Based on the measured values shown in Fig. 3 and concerning the relevant literature [33, 34], the elastic modulus at room temperature ( $E_{c,R}^{25}$ ) was used as the benchmark for normalizing and the elastic modulus ( $E_{c,R}^T$ ) of the specimen was fitted, as shown in Fig. 4.



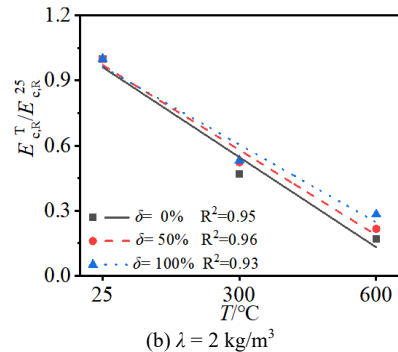
(a)  $\lambda = 0 \text{ kg/m}^3$



(b)  $\lambda = 2 \text{ kg/m}^3$



(a)  $\lambda = 0 \text{ kg/m}^3$



(b)  $\lambda = 2 \text{ kg/m}^3$

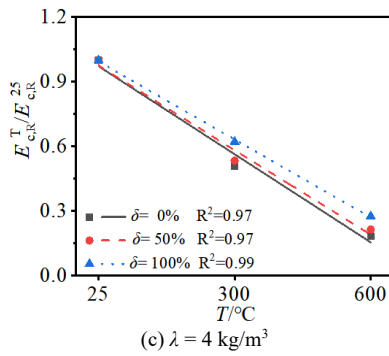


Fig. 4. Fitting curves of elastic modulus of specimens with different variation parameters.

Ordinary concrete's elastic modulus reduced more with increasing temperature than RAC, as illustrated in Fig. 4. This is because ordinary concrete has a higher elastic modulus at room temperature than RAC, therefore when temperature fluctuations cause damage to the elastic modulus of both RAC and ordinary concrete, the value of ordinary concrete declines faster. The elastic modulus increased linearly with temperature increase, and the functional relationship between the elastic modulus and other variation parameters was formed with the introduction of replacement ratio and fiber dosage influence factors, as indicated in Eq. (1). Among them, based on the measured data, it was found that the fiber dosage had almost no effect on the elastic modulus of the specimens, so the effect of fiber on the elastic modulus of the specimens was ignored.

$$E_{c,R}^T / E_{c,R}^{25} = 0.98 - (2\delta - 14)T \times 10^{-4} \quad R^2 = 0.98 \quad (1)$$

where  $\delta$  represents the replacement ratio of recycled coarse aggregate, and  $T$  represents a different temperature.  $0\% \leq \delta \leq 100\%$ ,  $25^\circ\text{C} \leq T \leq 600^\circ\text{C}$ .

#### 4.2 Poisson's ratio

Based on the measured Poisson's ratio, Fig. 5 depicts the range of change of Poisson's ratio of the specimens with temperature, fiber dosage, and replacement ratio.

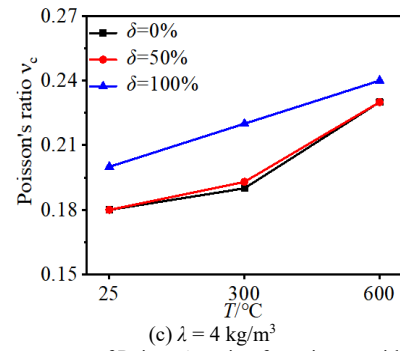
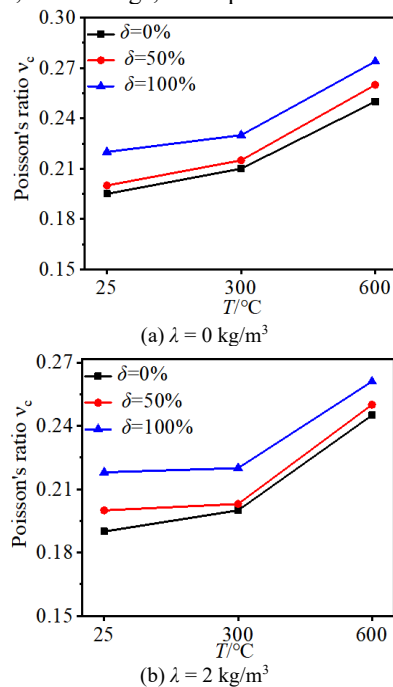


Fig. 5. Change range of Poisson's ratio of specimens with replacement ratio, fiber dosage, and temperature.

The Poisson's ratio of the specimens grew gradually higher with increasing temperature for the specimens with single parameter temperature fluctuation, as shown in Fig. 5. Under the same fiber dosage and replacement ratio, the increased range of Poisson's ratio was between 0.9% and 10% when the temperature was raised from 25 °C to 300 °C. When the temperature was raised from 300 °C to 600 °C, the increased range of Poisson's ratio was between 9% and 23.1%. Between 300 °C and 600 °C, the increase in Poisson's ratio was mostly concentrated. This is because the specimen's damage after 300°C high temperature is minor, however, the specimen's mortar after 600 °C high temperature is loose and multi-holed, and the aggregate's bond force is weakened, resulting in substantial lateral deformation under load.

The Poisson's ratio of the specimens showed an overall increasing tendency with the rise of replacement ratio for specimens with a single parameter change of replacement ratio. At the same temperature and fiber dosage, the increased range of Poisson's ratio was between 1.2% and 5.2% when the replacement ratio was increased from 0% to 50%. When the replacement ratio was increased from 50% to 100% , the increased range of Poisson's ratio was between 4% and 13.9%. The 100% recycled aggregate replacement ratio had the greatest effect on the Poisson's ratio when compared to the 50% replacement ratio. This is due to the recycled aggregate's high number of microcracks on the inside and old mortar on the outside, as well as its low overall rigidity. The steady accumulation of such initial faults causes the specimen's lateral deformation to increase, and the Poisson's ratio to rise.

The Poisson's ratio of the specimens reduced marginally as the BF dosage increased for specimens with a single parameter modification of fiber dosage. When the BF dosage was increased from 0 to 2 kg/m<sup>3</sup>, the Poisson's ratio of the specimens decreased from 0% to 5.5% at the same temperature and replacement ratio. When the BF dosage increased from 2 to 4 kg/m<sup>3</sup>, the Poisson's ratio decreased from 8% to 10% at the same temperature and replacement ratio. It is demonstrated that the tie effect of BF inside the RAC minimizes the specimen's lateral deformation to some amount. After individual specimens were combined with fibers, the Poisson's ratio of specimens did not alter among them. This could be due to the discrete nature of the RAC material. On the other hand, it could be due to the influence of high temperature, which weakens the bond force between the fiber and the mortar.

#### 5. Conclusions

Within the spectrum of design parameter modifications, BFRRC experimental tests on the deformation performance

of BFRRC after high temperature treatment were carried out in this study. The following are the main findings:

(1) For the single parameter variation of temperature, the elastic modulus of the specimen decreases significantly after the specimen has been exposed to high temperatures. For the variation of replacement ratio, the elastic modulus of the specimen decreases with the increasing of the replacement ratio. For the variation of fiber dosage, the elastic modulus of the specimen increases gradually with the increase of BF dosage, but the increase is not significant.

(2) For specimens with a single parameter change in temperature, the Poisson's ratio of the specimens progressively increases as the temperature rises, with the majority of the increase occurring between 300 °C and 600 °C. The Poisson's ratio shows an overall increasing trend with the increasing of replacement ratio, and the 100% replacement ratio of recycled aggregates has the largest effect on the Poisson's ratio when compared to the replacement ratio of 50%.

(3) The analytical expression of BFRRC elastic modulus and different variation parameters at high temperature is

established in this work via regression analysis, and it is in good accord with the experimental results.

The deformation performance of BFRRC after high temperature is related to the source and properties of RCA, further studies are necessary to reveal the influence law of RCA on the deformation performance. In addition, the general applicability of the established formula for elastic modulus needs to be further verified.

#### Acknowledgement

This work was financially supported by the Opening Funds of State Key Laboratory of Building Safety and Built Environment and National Engineering Research Center of Building Technology (BSBE2019-06), and the Key R & D and Promotion Projects in Henan Province (212102310288).

This is an Open Access article distributed under the terms of the Creative Commons Attribution License.



#### References

1. Akhtar, A., Sarmah, A. K., "Construction and demolition waste generation and properties of recycled aggregate concrete: A global perspective". *Journal of Cleaner Production*, 186, 2018, pp. 262-281.
2. Khushnood, R. A., Qureshi, Z. A., Shaheen, N., Ali, S., "Bio-mineralized self-healing recycled aggregate concrete for sustainable infrastructure". *Science of the Total Environment*, 703, 2020, pp. 135007.
3. Jin, R. Y., Li, B., Zhou, T. Y., Wanatowski, D., Piroozfar, P., "An empirical study of perceptions towards construction and demolition waste recycling and reuse in China". *Resources Conservation and Recycling*, 126, 2017, pp. 86-98.
4. Liew, K. M., Sojobi, A. O., Zhang, L. W., "Green concrete: Prospects and challenges". *Construction and Building Materials*, 156, 2017, pp. 1063-1095.
5. Safiuddin, M., Alengaram, U. J., Rahman, M. M., Salam, M. A., Jumaat, M. Z., "Use of recycled concrete aggregate in concrete: A review". *Journal of Civil Engineering and Management*, 19(6), 2013, pp. 796-810.
6. Pedro, D., de Brito, J., Evangelista, L., "Influence of the use of recycled concrete aggregates from different sources on structural concrete". *Construction and Building Materials*, 71, 2014, pp. 141-151.
7. Wang, S. R., Zhao, J. Q., Wu, X. G., Yang, J. H., Liu, A., "Meso-scale simulations of lightweight aggregate concrete under impact loading". *International Journal of Simulation Modelling*, 20(2), 2021, pp. 291-302.
8. Zhang, X. G., Wang, S. R., Gao, X., He, Y. S., "Seismic behavior analysis of recycled aggregate concrete-filled steel tube column". *Journal of Engineering Science and Technology Review*, 12(4), 2019, pp. 129-135.
9. Engelsen, C. J., van der Sloot, H. A., Petkovic, G., "Long-term leaching from recycled concrete aggregates applied as sub-base material in road construction". *Science of the Total Environment*, 587, 2017, pp. 94-101.
10. Mo, K. H., Ling, T. C., Alengaram, U. J., Yap, S. P., Yuen, C. W., "Overview of supplementary cementitious materials usage in lightweight aggregate concrete". *Construction and Building Materials*, 139, 2017, pp. 403-418.
11. Skarzynski, L., "Mechanical and radiation shielding properties of concrete reinforced with boron-basalt fibers using digital image correlation and x-ray micro-computed tomography". *Construction and Building Materials*, 255, 2020, pp. 119252.
12. Wang, S. R., Wu, X. G., Yang, J. H., Zhao, J. Q., Kong, F. L., "Mechanical behavior of lightweight concrete structures subjected to 3D coupled static-dynamic loads". *Acta Mechanica*, 231(11), 2020, pp. 4497-4511.
13. Marina, D., "Influence of reinforced concrete forming features on mechanical characteristics". *Technical Journal*, 13(2), 2019, pp. 86-91.
14. Zhang, X. G., Kuang, X. M., Wang, F., Wang, S. R., "Strength indices and conversion relations for basalt fiber-reinforced recycled aggregate concrete". *DYNA*, 94(1), 2019, pp. 82-87.
15. Ahmed, W., Lim, C. W., "Production of sustainable and structural fiber reinforced recycled aggregate concrete with improved fracture properties: A review". *Journal of Cleaner Production*, 279, 2021, pp. 123832.
16. Gao, D. Y., Zhu, W. W., Fang, D., Tang, J. Y., Zhu, H. T., "Shear behavior analysis and capacity prediction for the steel fiber reinforced concrete beam with recycled fine aggregate and recycled coarse aggregate". *Structures*, 37, 2022, pp. 44-55.
17. Liu, Z. Z., Lu, Y. Y., Li, S., Zong, S., Yi, S., "Flexural behavior of steel fiber reinforced self-stressing recycled aggregate concrete-filled steel tube". *Journal of Cleaner Production*, 274, 2020, pp. 122724.
18. Meesala, C. R., "Influence of different types of fiber on the properties of recycled aggregate concrete". *Structural Concrete*, 20(5), 2019, pp. 1656-1669.
19. Ali, B., Qureshi, L. A., Shah, S. H. A., Rehman, S. U., Hussain, I., Iqbal, M., "A step towards durable, ductile and sustainable concrete: Simultaneous incorporation of recycled aggregates, glass fiber and fly ash". *Construction and Building Materials*, 251, 2020, pp. 118980.
20. Xiong, Z., He, S. H., Kwan, A. K. H., Li, L. G., Zeng, Y., "Compressive behaviour of seawater sea-sand concrete containing glass fibres and expansive agents". *Construction and Building Materials*, 292, 2021, pp. 123309.
21. Samani, M. A., Lak, S. J., "Experimental investigation on the mechanical properties of recycled aggregate concrete reinforced by waste carbon fibers". *International Journal of Environmental Science and Technology*, 16(8), 2019, pp. 4519-4530.
22. Ding, H. J., Sun, Q. S., Wang, Y. Q., Jia, D. Z., Li, C. W., Ji, C., Feng, Y. P., "Flexural behavior of polyurethane concrete reinforced by carbon fiber grid". *Materials*, 14(18), 2021, pp. 5421.
23. Lee, S., "Effect of Nylon Fiber Addition on the Performance of Recycled Aggregate Concrete". *Applied Sciences-Basel*, 9(4), 2019, pp. 767.
24. Sainz-Aja, J. A., Sanchez, M., Gonzalez, L., Tamayo, P., del Angel, G. G., Aghajanian, A., Diego, S., Thomas, C., "Recycled polyethylene fibres for structural concrete". *Applied Sciences-Basel*, 12(6), 2022, pp. 2867.
25. Kim, S. B., Yi, N. H., Kim, H. Y., Kim, J. H. J., Song, Y. C., "Material and structural performance evaluation of recycled PET fiber reinforced concrete". *Cement & Concrete Composites*, 32(3), 2010, pp. 232-240.
26. Chen, X. F., Kou, S. C., Xing, F., "Mechanical and durable properties of chopped basalt fiber reinforced recycled aggregate concrete and the mathematical modeling". *Construction and Building Materials*, 298, 2021, pp. 123901.
27. Adesina, A., "Performance of cementitious composites reinforced with chopped basalt fibres-An overview". *Construction and Building Materials*, 266, 2021, pp. 120970.
28. Kabay, N., "Abrasion resistance and fracture energy of concretes with basalt fiber". *Construction and Building Materials*, 50, 2014, pp. 95-101.

29. Alnahhal, W., Aljidda, O., "Flexural behavior of basalt fiber reinforced concrete beams with recycled concrete coarse aggregates". *Construction and Building Materials*, 169, 2018, pp. 165-178.
30. Dong, J. F., Wang, Q. Y., Guan, Z. W., "Material properties of basalt fibre reinforced concrete made with recycled earthquake waste". *Construction and Building Materials*, 130, 2017, pp. 241- 251.
31. Zhang, C. S., Wang, Y. Z., Zhang, X. G., Ding, Y. H., Xu, P., "Mechanical properties and microstructure of basalt fiber-reinforced recycled concrete". *Journal of Cleaner Production*, 278, 2021, pp. 123252.
32. Huang, M., Zhao, Y. R., Wang, H. N., Lin, S. H., "Mechanical properties test and strength prediction on basalt fiber reinforced recycled concrete". *Advances in Civil Engineering*, 2021, pp. 6673416.
33. Chang, Y. F., Chen, Y. H., Sheu, M. S., Yao, G. C., "Residual stress - strain relationship for concrete after exposure to high temperatures". *Cement and Concrete Research*, 36(10), 2006, pp. 1999-2005.
34. Liu, Y. Z., Wang, W. J., Chen, Y. F., Ji, H. F., "Residual stress-strain relationship for thermal insulation concrete with recycled aggregate after high temperature exposure". *Construction and Building Materials*, 129, 2016, pp. 37-47.